buildings

MDPI

Article

Towards Sustainable Construction: Evaluating Thermal Conductivity in Advanced Foam Concrete Mixtures

Alireza Mohtadi [1,2], Mohammad Ghomeishi [3,*] and Ali Dehghanbanadaki [4,5]

[1] Department of Architecture, Gheshm Branch, Islamic Azad University, Gheshm 79515-1393, Iran; mohtadi@damavandiau.ac.ir
[2] Research and Development, Materials and Technology, Institute of Iran Concrete Clinic, Tehran 14738-63451, Iran
[3] Department of Architecture, Damavand Branch, Islamic Azad University, Tehran 39718-78911, Iran
[4] Department of Civil Engineering, Damavand Branch, Islamic Azad University, Damavand 39718-78911, Iran; a.dehghanbanadaki@damavandiau.ac.ir
[5] Research Center of Concrete and Soil, Damavand Branch, Islamic Azad University, Damavand 39718-78911, Iran
* Correspondence: ghomeishi.m@damavandiau.ac.ir

Abstract: Traditional concrete structures are frequently linked to poor energy efficiency and substantial heat loss, which pose significant environmental issues. To enhance thermal insulation and reduce heat loss, the use of precast insulated walls is suggested. This research introduces a new energy-efficient precast concrete panel (PCP). We explored various material combinations, including air bubbles, nano microsilica compound (NMC), nano microsilica powder (NMP), and latex, to determine the most effective formulation. A total of 99 tests were performed to assess the compressive strength of the samples, with 28 tests selected for thermal conductivity evaluations at temperatures of 300 °C and 400 °C based on satisfactory compressive strength results. The results indicated that the optimal mix of 4% air bubbles and 13% NMC achieved the lowest thermal conductivities of 1.31 W/m·K and 1.20 W/m·K at 300 °C and 400 °C, respectively, showing improvement ratios of 7% and 15.5% compared to the baseline tests. Additionally, the tests that included latex did not meet the thermal conductivity standards. The optimal combinations identified in this research can be effectively utilized in PCPs, resulting in significant energy savings. It is expected that stakeholders in the green building sector will recognize these proposed PCPs as a practical energy-efficient solution to advance sustainable and environmentally friendly construction practices.

Keywords: precast concrete panels; thermal insulation; energy efficiency

Citation: Mohtadi, A.; Ghomeishi, M.; Dehghanbanadaki, A. Towards Sustainable Construction: Evaluating Thermal Conductivity in Advanced Foam Concrete Mixtures. *Buildings* **2024**, *14*, 3636. https://doi.org/10.3390/buildings14113636

Academic Editor: Paulo Santos

Received: 19 October 2024
Revised: 7 November 2024
Accepted: 9 November 2024
Published: 15 November 2024

1. Introduction

Growing global energy and environmental concerns underscore the urgent need for energy efficiency, reduced emissions, and sustainable practices. In this regard, the building sector leads all industries as the top energy consumer and greenhouse gas emitter [1,2]. Residential buildings, as the most prevalent type of structure, demand greater focus to decrease their energy usage. The key to energy conservation in these buildings centers on upgrading the building envelope and heating systems [3]. In 2021, building operations alone were responsible for 30% of global energy consumption and 27% of emissions from the energy sector [4]. Consequently, there is an urgent need to reduce energy consumption in buildings. In this context, enhancing the thermal insulation of building elements such as walls and roofs can be highly effective [5]. Consequently, numerous energy efficiency rating systems and building codes mandate specific thermal resistance levels, especially in colder regions.

To improve the thermal performance of concrete, many researchers have conducted studies on the thermal and mechanical properties of concrete incorporating various additives, both in laboratory settings and at real-world scales [6–14]. For example, in the

research conducted by Ebru and Atmaca [15], Portland cement (PC) CEM II 42.5R was partially replaced with bentonite clay (BC) in varying proportions, ranging from 0 to 30% by volume. Mechanical and thermal conductivity tests were performed on the concrete samples after 28 days. Samples with 5% bentonite clay showed a substantial 94.7% improvement in compressive strength and a 31.2% decrease in thermal conductivity compared to the control group. However, exceeding 15% bentonite content significantly degraded both mechanical and thermal performance.

Air entrainment consistently proved more effective in lowering concrete's thermal conductivity than other explored additive modifications in small-scale tests [16–18]. For example, Abdellatief et al. [19] explored using eggshell powder (ESP) and sawdust ash (SDA), along with aluminum powder as a foaming agent, to create geopolymer foam concrete (GFC). Partially replacing precursors with up to 20% ESP and SDA, they found that a 10% ESP mix improved compressive strength by 16.54% and a 5% SDA mix by 4.45%, relative to the control mix. In terms of thermal performance, the 10% ESP mixture demonstrated a thermal conductivity of 1.237 W/m.K, which is significantly lower than that of conventional concrete, typically around 1.4–2.5 W/m.K, indicating improved insulation properties.

Beyond small-scale tests on the thermal behavior of concrete, various binders have been shown to positively influence the thermal performance of concrete in full-scale wall applications [20–24]. Moreover, numerical simulations were used to model the thermal behavior of concrete in different building configurations, offering detailed insights into how various factors impact heat transfer and insulation performance in real-world conditions [25–28]. These studies collectively demonstrate that alternative binders not only enhance thermal insulation properties, but also maintain the structural integrity of concrete, making them viable for practical construction applications. For example, Ding et al. [29] developed prefabricated lightweight self-insulating foamed concrete wall panels using low-density, thermally insulating foamed concrete. While the panels' impermeability met Chinese standards, their dry shrinkage, though improved, remained suboptimal. Crucially, the 150 mm thick panels exhibited excellent mechanical properties, meeting or exceeding standards for flexural strength, impact resistance, and load-bearing capacity, suggesting their suitability for enhancing building insulation and structural performance.

Two studies explored the enhancement of building insulation using modified foamed concrete. Nguyen-Van et al. [22] incorporated phase-change materials (PCM) into foamed concrete cladding panels, significantly reducing internal wall and air temperatures, although the performance varied with sun exposure. Shi et al. [30] investigated using desert sand (DS) and rice husk ash (RHA) in foamed concrete. While DS improved stability but reduced strength, adding RHA mitigated this by enhancing the matrix structure and thermal performance. The DS/RHA combination improved insulation, lowered environmental impact, and reduced costs. Both studies demonstrate promising approaches to improving building energy efficiency with modified foamed concrete.

Despite significant advancements in building materials and energy efficiency, there remains a critical need to further enhance energy savings in concrete structures. Numerous studies have been published highlighting various approaches to this challenge [8,31–38]; however, innovative solutions are still required to optimize thermal performance. This study aims to contribute to this ongoing effort by focusing on the development of a novel concrete panel specifically designed for interior walls, with the goal of improving energy efficiency in buildings. The primary objective of this study is to develop a new precast concrete panel (PCP) that enhances energy efficiency. To achieve this, the research will evaluate the effects of various combinations of cement dosages, air bubbles, nano microsilica compound (NMC), nano microsilica powder (NMP), and latex on the thermal conductivity of the PCP. The ultimate goal is to reduce the thermal conductivity of the lightweight concrete panel while ensuring that the material maintains an acceptable level of compressive strength.

2. Experimental Design

2.1. Used Materials and Testing Program

A new concrete panel has been developed and proposed for use in buildings situated in cold regions. This study involved the production of samples utilizing various combinations of cement dosages, air bubbles, NMC, NMP, and latex for compressive and thermal testing.

The selection of specific ingredients for developing the concrete mixture was based on their unique properties and potential synergistic effects in achieving both thermal efficiency and structural integrity. The incorporation of NMC and NMP was primarily driven by their nanoscale particle size, which enables them to fill microscopic voids in the cement matrix, creating a denser microstructure. Their high surface area-to-volume ratio enhances reactivity with cement compounds, promoting stronger chemical bonds through pozzolanic reactions that produce additional C-S-H gel. Similarly, air bubbles were introduced through foaming agents to create a cellular structure within the concrete matrix that traps air, naturally reducing thermal conductivity while decreasing the overall density of the concrete panel. This combination of nanomaterials and air voids was designed to optimize thermal resistance while maintaining structural integrity.

The inclusion of latex in certain mix designs was aimed at improving the bond between cement particles and aggregates while enhancing the flexibility and crack resistance of the hardened concrete. This additive also contributes to reduced permeability, which can affect thermal properties, and provides better adhesion properties for potential surface treatments. The systematic selection and combination of these materials directly aligned with our research objectives of developing energy-efficient precast concrete panels while maintaining structural requirements for interior wall applications. Through varying proportions of these materials in different mix designs, we were able to identify the optimal combination that achieves the lowest thermal conductivity while meeting the required compressive strength criteria, making these panels particularly suitable for interior wall applications in buildings situated in cold regions.

Figure 1 illustrates the materials and the proposed concrete panel utilized in this research. The primary investigation focused on evaluating the effects of these materials on the compressive strength of the samples. Both the individual and combined effects of these materials were tested. The concrete mix design is presented in Table 1. The engineering properties of used materials are shown in Table 2. The exact details of these tests, including the specific percentages of each additive, are shown in Table A1 (Appendix A). Based on Table A1, 99 tests (TS-1 to TS-99) were conducted. It should be noted that the effects of these materials were only evaluated using samples cured for 28 days. As expected, the inclusion of air bubbles decreased the compressive strength of the samples. Therefore, thermal conductivity tests were only performed on selected samples that met the minimum required compressive strength. This selection will be discussed in the Results section.

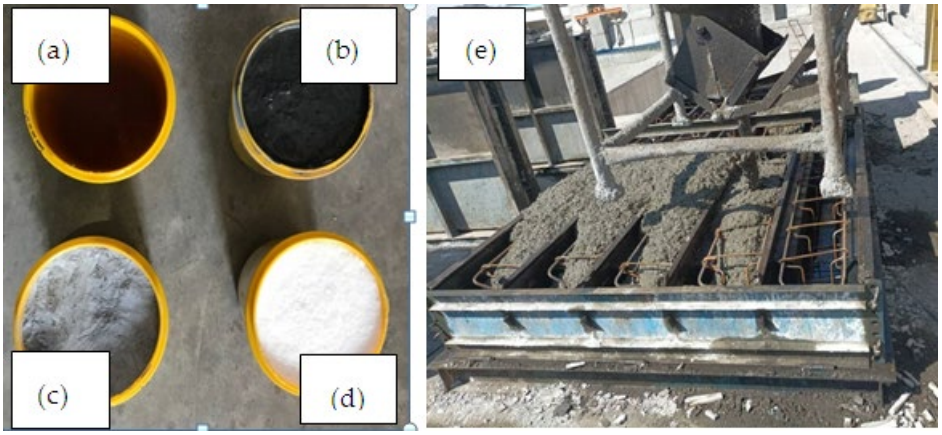

Figure 1. Materials used for the tests. (**a**) Air bubble, (**b**) NMC, (**c**) NMP, (**d**) latex, (**e**) PCP.

Table 1. Concrete mix design.

Reference Mixture	Cement Dosage (kg/m^3)	W/C	W (kg)	C (kg)	G (Natural Coarse)	S (Fine Coarse)
I	300	0.5	150	300	1135	730
II	350	0.5	175	350	1140	745
III	400	0.5	200	400	1160	756

Note: W/C = water to cement; C = cement; G = gravel; S = sand.

Table 2. Engineering properties of used materials.

Properties	NMC	NMP	Latex
Particle Size	0.3 µm	50 nm	100 nm
Density	2.2 g/cm^3	2.4 g/cm^3	1.1 g/cm^3

2.2. Implementation of Precast Concrete Panels for Interior Wall Systems

The thermally-efficient PCPs developed in this research are particularly suitable for interior wall applications, offering both thermal insulation and space-efficient solutions for building interiors. This section outlines the practical implementation aspects of these panels as interior wall systems. Interior PCPs primarily utilize two types of connections: floor/ceiling connections and panel-to-panel connections. The floor connection system employs L-shaped steel brackets anchored to the floor slab, allowing for vertical adjustment during installation. At the ceiling interface, adjustable top connections accommodate construction tolerances and potential floor deflection. Panel-to-panel connections are achieved through concealed mechanical fasteners or tongue-and-groove systems, ensuring smooth wall surfaces while maintaining thermal properties. This approach to interior PCP implementation combines the thermal efficiency benefits of our research with practical installation considerations, supporting sustainable interior construction practices while maintaining functionality and esthetics.

2.3. Test Standards

The experimental procedures adhered to specific standards for both the preparation and testing of the samples. The ASTM standard C260-86 (1995) [39] was followed for the suggested combinations and proportions of additives used in the concrete mixtures. This standard outlines the requirements for air-entraining admixtures used in concrete, which are chemical additives that introduce and stabilize microscopic air bubbles in the concrete mix. For evaluating the compressive strength of the samples, the BS EN 12390-3 standard (2009) [40] was employed. This standard outlines the methods for making and curing test specimens, as well as the procedures for conducting the compressive strength tests.

The thermal conductivity coefficient of the samples was tested according to the ISO 8301 standard (1991) [41], which specifies the use of the guarded hot plate apparatus for determining the steady-state thermal transmission properties of materials. The apparatus consists of a central heating plate, surrounded by a guard ring, and two cooling plates, ensuring a uniform one-dimensional heat flow through the sample. The test specimens were placed between the hot and cold plates and the heat flux through the material was measured. The thermal conductivity was calculated based on the temperature gradient and the heat flow across the sample. For this study, measurements were carried out at two distinct temperature levels, 300 °C and 400 °C, to evaluate the material's performance under varying thermal conditions. The apparatus was calibrated and maintained according to the ISO 8301 (1991) [41] guidelines to ensure the accuracy and repeatability of the results. Figure 2a,b illustrate the compressive strength and thermal conductivity tests conducted in this study, respectively.

(**a**)

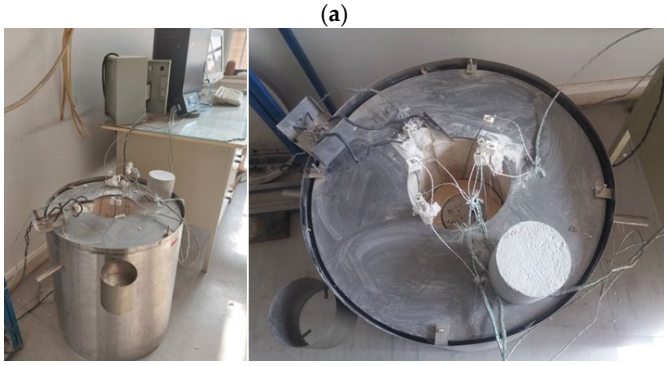

(**b**)

Figure 2. Experimental tests. (**a**) Compressive strength test; (**b**) thermal conductivity test.

A petrographic analysis was conducted on hardened concrete samples to assess the air-void system, specifically to characterize the size, distribution, and morphology of the air bubbles within the cement paste. This analysis provided quantitative data on air content and void characteristics, which are crucial factors influencing the freeze–thaw durability and overall performance of the concrete. Thin sections were prepared and examined under a polarized microscope to identify and measure the air voids, allowing for a detailed assessment of the air-entraining admixture's effectiveness and the resulting air-void system's characteristics.

3. Results and Discussions

3.1. Compressive Strength Tests

Figure 3a,b illustrate the compressive strength (f'c) results from the conducted tests. The baseline test, which utilized 300 kg/m^3 of cement without any additives, achieved an f'c of 35.53 MPa. It is well established that the incorporation of air bubbles generally reduces f'c. For instance, the addition of 4% air (designated as TS-5) to the baseline mixture, without any other additives, resulted in a significant decrease in compressive strength to 15.77 MPa, reflecting a reduction of approximately 55%. Conversely, in the TS-9 test, the incorporation of 8% NMC led to an increase in f'c to 40.33 MPa, demonstrating an improvement of 13%. Additionally, Figure 3a presents the top four tests ranked by f'c. Notably, the highest f'c was observed in the TS-72 test, which utilized a combination of 5% NMC, achieving an f'c of 56.83 MPa.

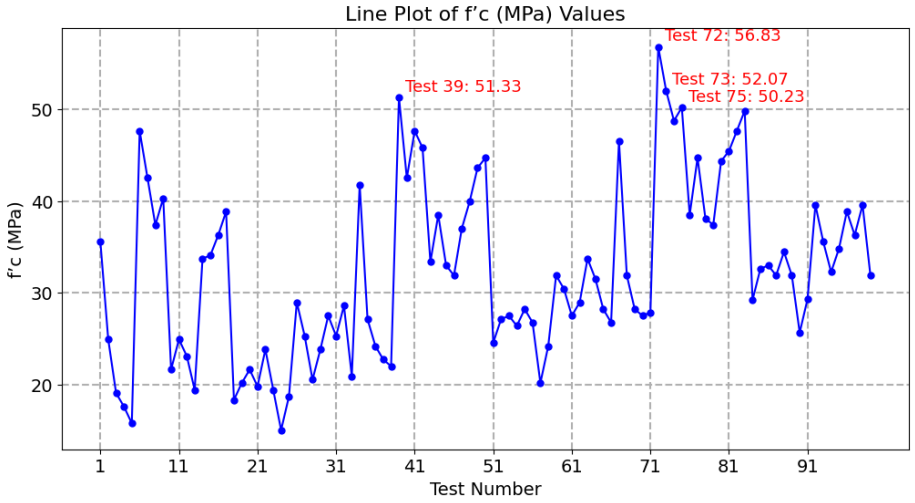

(**a**)

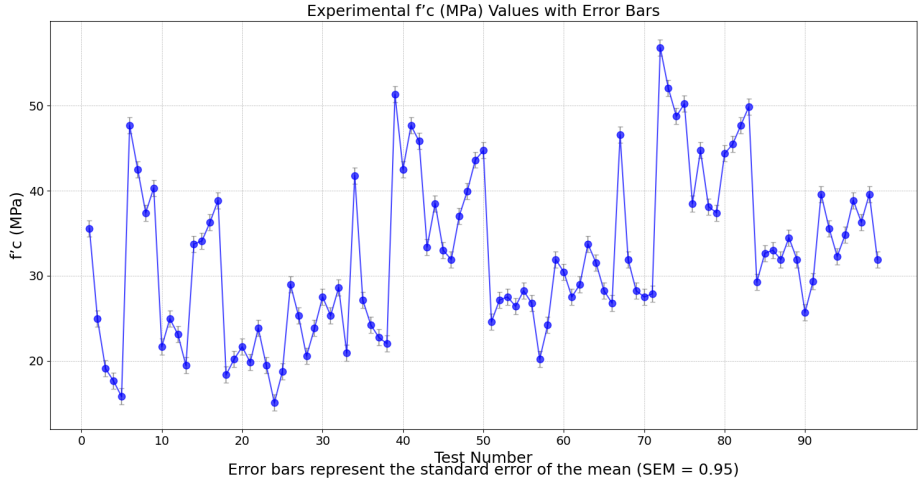

(**b**)

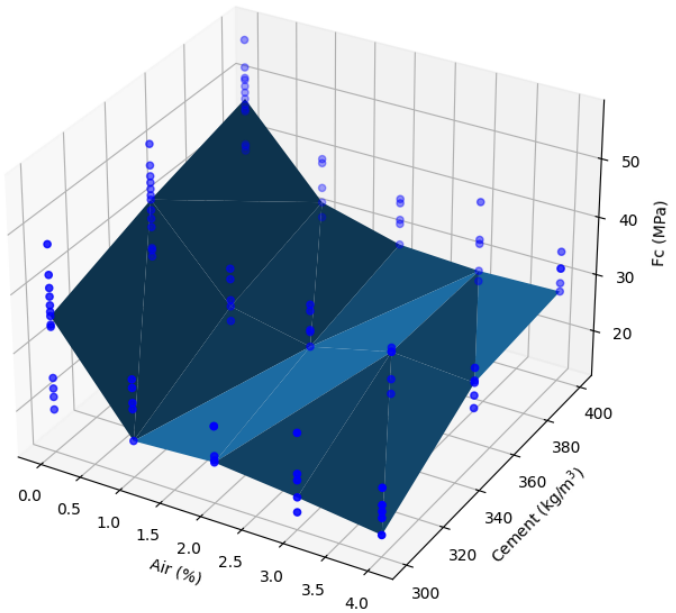

(**c**)

Figure 3. (**a**) f'c of the tests. (**b**) Error bar of the f'c; (**c**) 3D chart for the f'c.

For better visualization, Figure 3c presents the f'c values in a 3D format. As expected, reducing the air content and increasing the cement quantity generally led to higher f'c values. However, the presence of the NMC and NMP in some test combinations reveals that the addition of air can actually enhance f'c. This unexpected outcome is attributed to the beneficial effects of NMC and NMP. Nevertheless, due to the influence of four distinct parameters, achieving precise visualization and interpretation of the results, even in a 3D format, remains challenging.

To better illustrate the influence of various parameters on f'c, a correlation matrix of the developed dataset was generated and is presented in Figure 4. Given the complex interactions among the influencing parameters, this chart provides an approximate representation of their effects on the f'c of the samples. As expected, the results indicate a positive correlation between cement content and f'c, while latex exhibits a negative impact on f'c. The reduction in f'c associated with latex-modified concrete can be attributed to several factors. First, latex tends to increase the flexibility of the concrete compared to conventional mixes. While this flexibility enhances crack resistance and improves toughness, it may also lead to lower f'c, especially if the mix is primarily designed for flexibility rather than load-bearing capacity. Additionally, the introduction of latex can result in increased air entrapment within the concrete mix, which further contributes to a decrease in f'c.

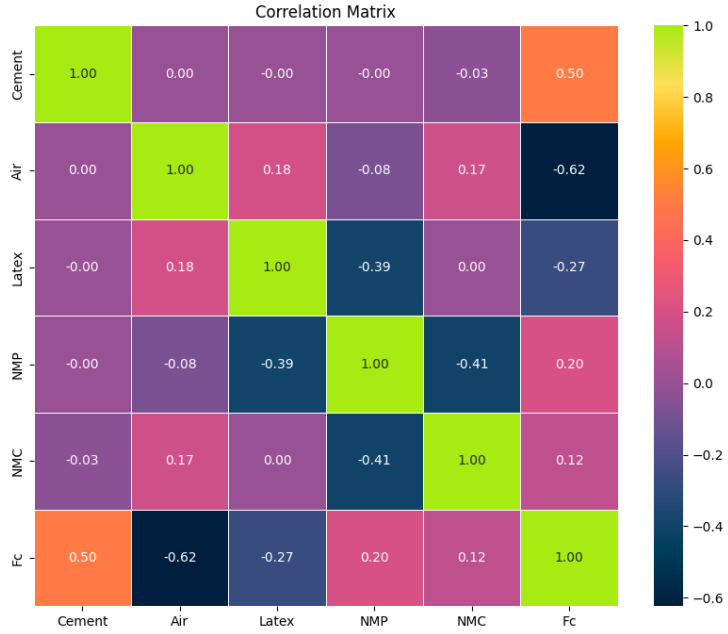

Figure 4. Correlation between effective parameters for estimating the f'c.

The correlation matrix indicates positive correlations for both the NMC and NMP with values of 0.12 and 0.20, respectively. These positive correlations suggest that the inclusion of these materials enhances the f'c of the concrete samples. The beneficial effects of NMC and NMP can be attributed to their ability to improve the microstructure of the concrete. Specifically, these nano-sized materials fill the voids within the cement matrix, leading to a denser and more homogeneous structure. This densification reduces the porosity of the concrete, which, in turn, enhances its mechanical properties, including f'c. Additionally, both NMC and NMP contribute to the pozzolanic reaction, which further enhances strength by producing additional calcium silicate hydrates (C-S-H) during hydration. This reaction not only improves the binding properties of the concrete, but also contributes to increased durability and resistance to environmental factors, making these materials valuable additives in the pursuit of higher f'c.

It should be mentioned that NMP outperforms NMC in enhancing the f'c due to its finer particle size, which allows for better void filling and improved packing density within the concrete matrix. NMP exhibits higher pozzolanic reactivity, leading to the

greater production of calcium silicate hydrate (C-S-H) during hydration. Additionally, NMP contributes less to air entrapment, resulting in a denser mix. Its superior workability facilitates more uniform material distribution, enhancing the overall concrete performance. These factors collectively make NMP a more effective additive for achieving higher f'c.

3.2. Thermal Conductivity Tests

Figure 5a–c depict the thermal conductivity of the test samples across various conditions. Based on these results, the thermal conductivity and f'c of various PCP mixtures at 300 °C were analyzed in relation to different material compositions. The thermal conductivity (K) values were found to range from 1.20 W/m·K to 2.12 W/m·K, while the f'c varied between 15.77 MPa and 46.57 MPa. These variations are attributed to the influence of cement content, air entrainment, latex, NMP, and NMC.

The effect of air entrainment on the thermal and mechanical properties was particularly evident. Samples containing air (e.g., TS-5, TS-21, TS-29) exhibited lower thermal conductivity values, as air acts as an effective insulator. For instance, TS-5, which contained 4% air, showed a thermal conductivity of 1.28 W/m·K, one of the lowest values recorded. However, this reduction in thermal conductivity was accompanied by a significant decrease in f'c, with TS-5 exhibiting the lowest f'c of 15.77 MPa. This suggests that while air entrainment improves thermal insulation, it has a detrimental effect on the mechanical strength of the concrete.

The inclusion of latex in the mixtures was found to increase thermal conductivity, but it also enhanced compressive strength. For example, TS-66, which contained 5% latex, exhibited a thermal conductivity of 2.02 W/m·K, higher than most other samples. Despite this, the compressive strength of TS-66 remained relatively high at 26.77 MPa. Similarly, TS-99, which also contained 5% latex, displayed the highest thermal conductivity at 2.12 W/m·K, but still maintained a compressive strength of 31.9 MPa. These results indicate that latex improves the mechanical performance of the concrete, albeit at the cost of increased thermal conductivity.

The effects of NMC on both thermal and mechanical properties were also significant. Samples containing NMC (e.g., TS-21, TS-33, TS-54, TS-66, TS-87, TS-99) generally exhibited higher thermal conductivity values. For instance, TS-99, which contained 8% NMC, showed the highest thermal conductivity of 2.12 W/m·K. However, its f'c was also relatively high at 31.9 MPa, suggesting that the use of NMC enhances the mechanical properties of the concrete, albeit with an associated increase in thermal conductivity. This trend was consistent across other samples containing NMC, such as TS-33 and TS-66, both of which exhibited high thermal conductivity but maintained good f'c.

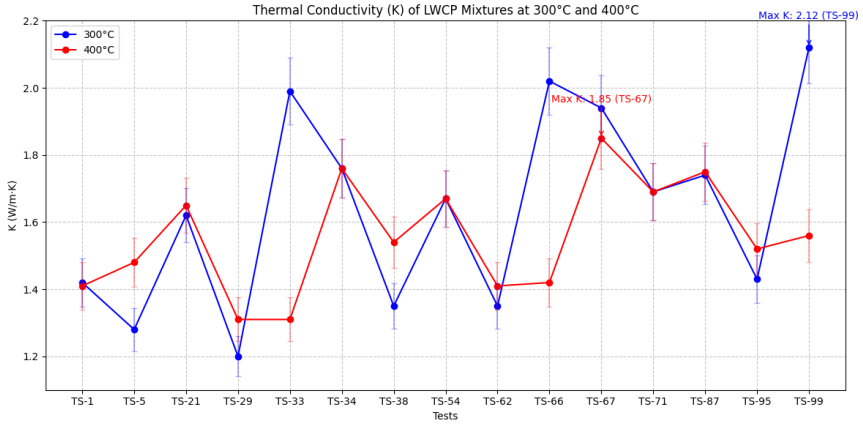

(**a**)

Figure 5. *Cont.*

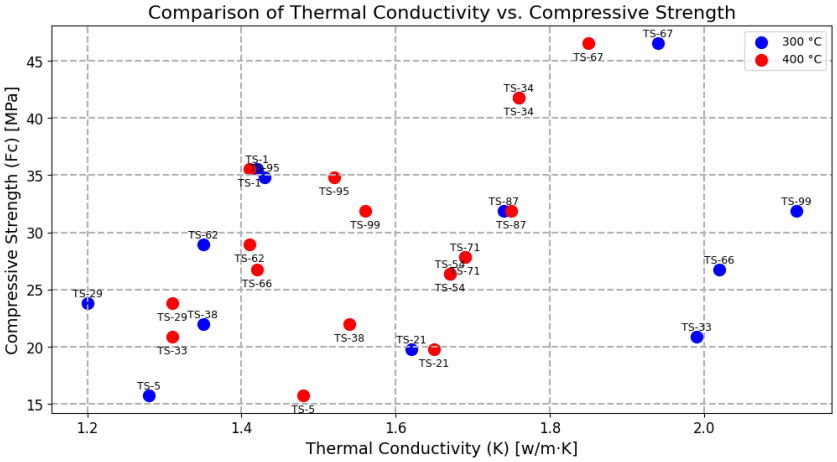

(**b**)

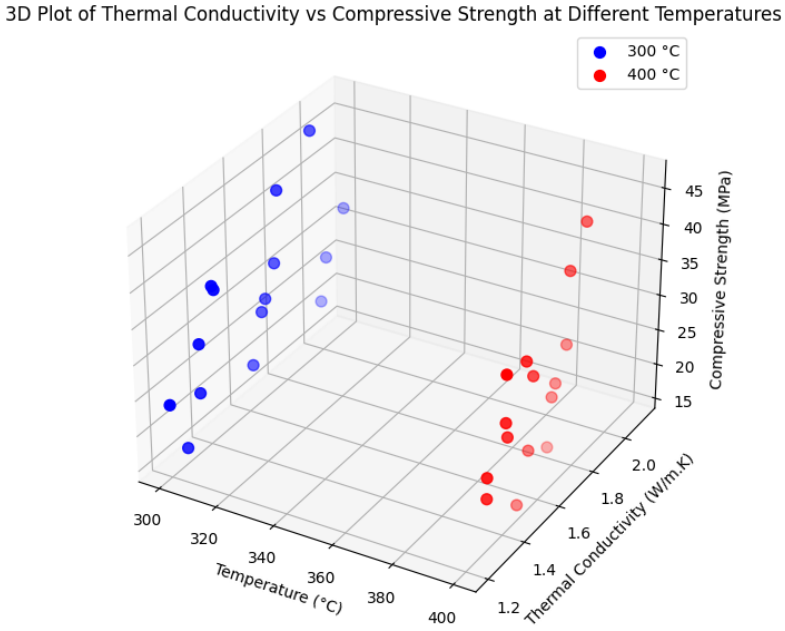

(**c**)

Figure 5. (**a**) Thermal conductivity of the tests. (**b**) Compressive vs. thermal conductivity; (**c**) 3D data.

3.3. Improvement Ratio of the Thermal Conductivity Tests

The analysis of the improvement rates of thermal conductivity for selected tests, as depicted in Figure 6, highlights significant findings. Tests TS-5, TS-29, TS-33, TS-38, and TS-62 showed notable reductions in thermal conductivity compared to the baseline. Among these, TS-29 demonstrated exceptional performance, with the optimal combination of 4% air bubbles and 13% NMP, achieving the lowest thermal conductivities of 1.31 W/m·K at 300 °C and 1.20 W/m·K at 400 °C. These changes resulted in improvement ratios of 7% and 15.5%, respectively, compared to the baseline. The graph illustrates that the selected tests generally achieved better improvement ratios at 400 °C than at 300 °C, indicating enhanced thermal performance at higher temperatures. This trend underscores the effectiveness of the material modifications in maintaining lower thermal conductivity under elevated thermal conditions.

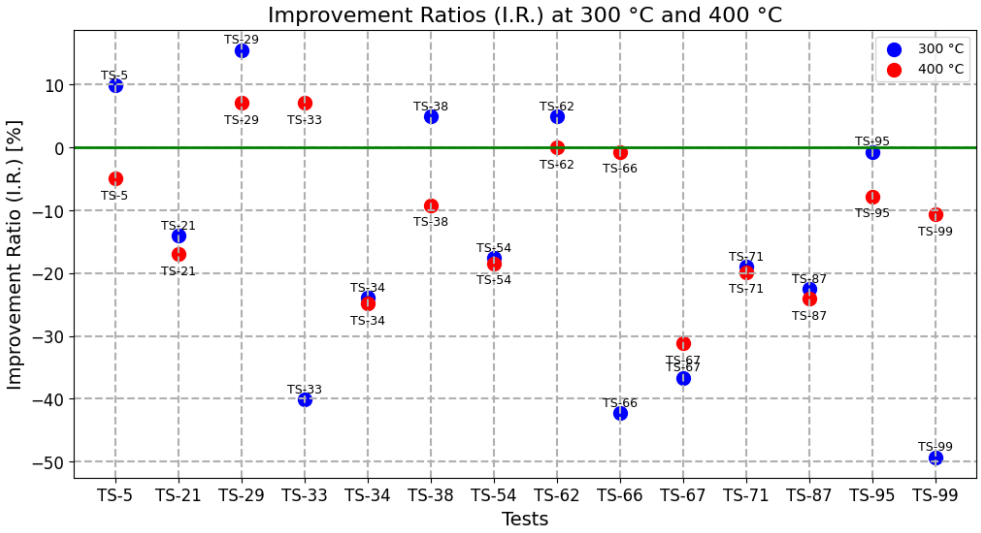

Figure 6. Improvement ratio of the thermal conductivity of the tests.

Additionally, it was observed that tests incorporating latex did not meet the desired thermal conductivity requirements, suggesting that latex may not be suitable for applications prioritizing thermal insulation. This insight directs future research towards exploring alternative additives that might better balance thermal and mechanical properties. The findings suggest that the optimal combinations identified, particularly those in TS-29, can be effectively applied in precast concrete panels, offering potential for significant energy savings. The application of these optimized mixtures in construction could lead to improved energy efficiency in buildings, aligning with sustainable development goals. Further research could explore scaling these findings to real-world applications, considering long-term performance and cost-effectiveness.

Figure 7 depicts the microstructure of the concrete samples, specifically highlighting the distribution and characteristics of air bubbles within the matrix. The petrographic analysis of the TS-5 sample, which contains 4% air, reveals the presence and arrangement of air voids throughout the concrete structure. These air bubbles, indicated by red dots in the image, play a crucial role in the thermal performance of the concrete panel. The distribution, size, and frequency of these air voids directly influence the material's thermal conductivity by creating discontinuities in the solid matrix that impede heat transfer.

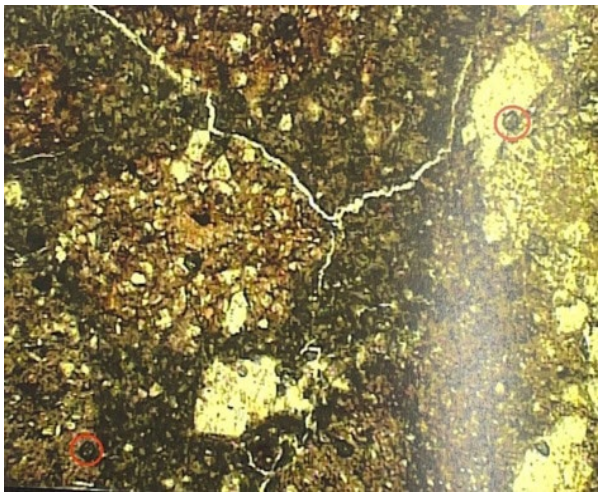

Figure 7. Petrographic analysis of concrete samples, highlighting air bubbles.

The petrographic analysis shown in Figure 7 allows for a detailed examination of the concrete's internal structure, providing visual evidence of the effectiveness of the air

entrainment process. The presence of these air bubbles contributes to the lightweight nature of the concrete and its improved insulating properties. This microscopic view of the concrete sample supports our findings regarding the thermal conductivity improvements observed in the TS-5 mix design, demonstrating the correlation between the intentional introduction of air voids and the enhanced thermal performance of the precast concrete panels. Furthermore, this analysis helps validate the methodology employed in creating energy-efficient concrete mixtures for interior wall applications.

3.4. Energy Saving Estimation

To demonstrate the potential energy savings of the optimized precast concrete panels (PCPs), we present a comparative analysis using a hypothetical building scenario. This example illustrates the energy savings achieved by using our most effective mixture (TS-29) compared to a standard concrete panel.

Example Scenario:

Consider a 10-story office building located in a cold climate region, with each floor having 1000 m^2 of floor area. The building has 4000 m^2 of interior walls made of precast concrete panels, with a thickness of 0.15 m.

Calculation Method:

Heat Transfer Equation: $Q = k \times A \times (\Delta T/d)$
where:
Q = Heat transfer rate (W)
k = Thermal conductivity (W/m·K)
A = Surface area (m^2)
ΔT = Temperature difference (K)
d = Wall thickness (m)
Assumptions:

Indoor temperature: 20 °C
Average outdoor temperature during heating season: 0 °C
Heating season duration: 180 days

Comparison:

(a) Standard concrete panel: k = 1.42 W/m·K (baseline value)
(b) Optimized PCP (TS-29): k = 1.20 W/m·K

Calculations:
Heat transfer rate for standard panel:
$Q\_std = 1.42 \times 4000 \times (20/0.15) = 756{,}800$ W
Heat transfer rate for optimized PCP:
$Q\_opt = 1.20 \times 4000 \times (20/0.15) = 640{,}000$ W
Energy Savings:
Daily energy saving: (756,800–640,000) × 24 h = 2,803,200 Wh = 2803.2 kWh
Seasonal energy saving: 2803.2 kWh × 180 days = 504,576 kWh
Cost Savings:
Assuming an electricity cost of USD 0.12 per kWh:
Annual cost saving: 504,576 kWh × USD 0.12 = USD 60,549.12

This example demonstrates that using the optimized PCP (TS-29) could potentially save approximately 504,576 kWh of energy per heating season, translating to a cost saving of over USD 60,000 annually for this hypothetical building. This represents a significant reduction in energy consumption and operational costs, highlighting the practical benefits of the developed PCPs in building applications.

It is important to note that the actual savings may vary depending on specific building characteristics, climate conditions, and energy prices. However, this example clearly illustrates the substantial potential for energy and cost savings when implementing the optimized precast concrete panels developed in this study.

4. Conclusions

This study investigated the optimization of concrete mixture designs for enhanced thermal performance in precast concrete panels (PCPs), balancing the need for both low thermal conductivity and adequate compressive strength. A total of 99 initial mixes were tested, with 28 selected for further thermal analysis. The key findings are summarized below.

- The most effective mixture (TS-29) incorporated 4% air bubbles and 13% nano microsilica powder (NMP), achieving thermal conductivities of 1.31 W/m·K and 1.20 W/m·K at 300 °C and 400 °C, respectively. This represents a 7% and 15.5% improvement compared to the baseline, demonstrating significant potential for energy savings in building applications.
- While air entrainment effectively reduced thermal conductivity, it also lowered compressive strength. This highlights the importance of carefully balancing air content to achieve optimal performance in both areas.
- Latex addition, while beneficial for compressive strength, proved detrimental to thermal insulation, increasing conductivity. This suggests latex is unsuitable for PCP applications where thermal performance is a primary concern.
- Nano microsilica compound (NMC) additions exhibited a complex relationship with both thermal conductivity and compressive strength, generally increasing both. Further investigation is warranted to fully understand the influence of NMC on overall PCP performance.

5. Limitations of the Current Study and Recommendations for Future Research

It should be mentioned that, in the present study, the material exploration focused on a specific set of components (air bubbles, NMC, NMP, and latex), potentially overlooking other promising additives. Furthermore, the research was conducted under controlled laboratory conditions, necessitating further investigation into real-world applications and long-term performance. The study primarily evaluated compressive strength, neglecting other important mechanical properties like flexural strength and impact resistance. Finally, a comprehensive cost analysis was not included, limiting the assessment of economic viability.

Building upon the findings of this study, several recommendations for future research emerge. Expanding the material investigation to include a broader range of additives, such as different nanoparticles, fibers, and supplementary cementitious materials, could further enhance PCP performance. Validating the laboratory findings through field studies and pilot projects is crucial for assessing real-world durability and performance. A more comprehensive mechanical testing program, incorporating flexural strength, impact resistance, and other relevant properties, is needed. Finally, life-cycle assessment and cost–benefit analysis are essential for evaluating the environmental and economic impacts of the optimized PCPs, paving the way for their wider adoption in sustainable construction.

While our innovative precast concrete panel design offers significant thermal performance benefits, it is important to acknowledge certain constraints. The incorporation of the nano microsilica compound may result in marginally increased upfront costs. Additionally, the manufacturing process requires the meticulous management of air content to achieve optimal results. Nevertheless, these challenges are outweighed by the considerable enhancements in thermal insulation and long-term energy conservation. The design's alignment with sustainable building practices and its potential for widespread application in energy-conscious construction make it a valuable contribution to the field. Despite the initial complexities, the design maintains feasibility for practical implementation, striking a balance between advanced performance and real-world applicability in the construction industry.

To build upon the results of this study, we propose implementing extensive energy simulations using sophisticated modeling software like EnergyPlus. Our research primarily concentrated on the experimental creation and evaluation of novel precast concrete panels. However, incorporating comprehensive energy simulations would offer crucial information about the extended performance of these panels in diverse real-world applications. Such

simulations would enhance our understanding of the panels' effectiveness across various building types and climate zones and over extended time periods, thereby providing a more complete picture of their potential impact on energy efficiency in the construction industry.

Further research should also consider optimizing PCP designs for specific climate zones to maximize energy efficiency.

Author Contributions: Methodology, A.M.; Writing—original draft, A.M.; Visualization, A.D.; Supervision, M.G. and A.D. All authors have read and agreed to the published version of the manuscript.

Funding: This research received no external funding.

Data Availability Statement: The original contributions presented in the study are included in the article, further inquiries can be directed to the corresponding author.

Conflicts of Interest: The authors declare no conflicts of interest.

Appendix A

Table A1. Details of the compressive strength tests.

Test	Cement Dosage	Additives	Additive Percentage (%)
TS-1	300	None	0
TS-2	300	Air bubbles	1
TS-3	300	Air bubbles	2
TS-4	300	Air bubbles	3
TS-5	300	Air bubbles	4
TS-6	300	NMC	5
TS-7	300	NMC	6
TS-8	300	NMC	7
TS-9	300	NMC	8
TS-10	300	Latex	2
TS-11	300	Latex	3
TS-12	300	Latex	4
TS-13	300	Latex	5
TS-14	300	NMP	10
TS-15	300	NMP	11
TS-16	300	NMP	12
TS-17	300	NMP	13
TS-18	300	Air bubbles and NMC	1–5
TS-19	300	Air bubbles and NMC	2–6
TS-20	300	Air bubbles and NMC	3–7
TS-21	300	Air bubbles and NMC	3–8
TS-22	300	Air bubbles and Latex	1–2
TS-23	300	Air bubbles and Latex	2–3
TS-24	300	Air bubbles and Latex	3–4
TS-25	300	Air bubbles and Latex	4–5

Table A1. *Cont.*

Test	Cement Dosage	Additives	Additive Percentage (%)
TS-26	300	Air bubbles and NMP	1–10
TS-27	300	Air bubbles and NMP	2–11
TS-28	300	Air bubbles and NMP	3–12
TS-29	300	Air bubbles and NMP	4–13
TS-30	300	Air bubbles, NMC, and Latex	1–5–2
TS-31	300	Air bubbles, NMC, and Latex	2–6–3
TS-32	300	Air bubbles, NMC, and Latex	3–7–4
TS-33	300	Air bubbles, NMC, and Latex	4–8–5
TS-34	350	None	0
TS-35	350	Air bubbles	1
TS-36	350	Air bubbles	2
TS-37	350	Air bubbles	3
TS-38	350	Air bubbles	4
TS-39	350	NMC	5
TS-40	350	NMC	6
TS-41	350	NMC	7
TS-42	350	NMC	8
TS-43	350	Latex	2
TS-44	350	Latex	3
TS-45	350	Latex	4
TS-46	350	Latex	5
TS-47	350	NMP	10
TS-48	350	NMP	11
TS-49	350	NMP	12
TS-50	350	NMP	13
TS-51	350	Air bubbles and NMC	1–5
TS-52	350	Air bubbles and NMC	2–6
TS-53	350	Air bubbles and NMC	3–7
TS-54	350	Air bubbles and NMC	3–8
TS-55	350	Air bubbles and Latex	1–2
TS-56	350	Air bubbles and Latex	2–3
TS-57	350	Air bubbles and Latex	3–4
TS-58	350	Air bubbles and Latex	4–5
TS-59	350	Air bubbles and NMP	1–10
TS-60	350	Air bubbles and NMP	2–11
TS-61	350	Air bubbles and NMP	3–12
TS-62	350	Air bubbles and NMP	4–13
TS-63	350	Air bubbles, NMC, and Latex	1–5–2
TS-64	350	Air bubbles, NMC, and Latex	2–6–3

Table A1. *Cont.*

Test	Cement Dosage	Additives	Additive Percentage (%)
TS-65	350	Air bubbles, NMC, and Latex	3–7–4
TS-66	350	Air bubbles, NMC, and Latex	4–8–5
TS-67	400	None	0
TS-68	400	Air bubbles	1
TS-69	400	Air bubbles	2
TS-70	400	Air bubbles	3
TS-71	400	Air bubbles	4
TS-72	400	NMC	5
TS-73	400	NMC	6
TS-74	400	NMC	7
TS-75	400	NMC	8
TS-76	400	Latex	2
TS-77	400	Latex	3
TS-78	400	Latex	4
TS-79	400	Latex	5
TS-80	400	NMP	10
TS-81	400	NMP	11
TS-82	400	NMP	12
TS-83	400	NMP	13
TS-84	400	Air bubbles and NMC	1–5
TS-85	400	Air bubbles and NMC	2–6
TS-86	400	Air bubbles and NMC	3–7
TS-87	400	Air bubbles and NMC	3–8
TS-88	400	Air bubbles and Latex	1–2
TS-89	400	Air bubbles and Latex	2–3
TS-90	400	Air bubbles and Latex	3–4
TS-91	400	Air bubbles and Latex	4–5
TS-92	400	Air bubbles and NMP	1–10
TS-93	400	Air bubbles and NMP	2–11
TS-94	400	Air bubbles and NMP	3–12
TS-95	400	Air bubbles and NMP	4–13
TS-96	400	Air bubbles, NMC, and Latex	1–5–2
TS-97	400	Air bubbles, NMC, and Latex	2–6–3
TS-98	400	Air bubbles, NMC, and Latex	3–7–4
TS-99	400	Air bubbles, NMC, and Latex	4–8–5

References

1. Zhang, Y.; Teoh, B.K.; Wu, M.; Chen, J.; Zhang, L. Data-Driven Estimation of Building Energy Consumption and GHG Emissions Using Explainable Artificial Intelligence. *Energy* **2023**, *262*, 125468. [CrossRef]
2. Gursel, A.P.; Shehabi, A.; Horvath, A. Embodied Energy and Greenhouse Gas Emission Trends from Major Construction Materials of US Office Buildings Constructed After the Mid-1940s. *Build. Environ.* **2023**, *234*, 110196. [CrossRef]

3. Osman, M.; Saad, M.M.; Ouf, M.; Eicker, U. From Buildings to Cities: How Household Demographics Shape Demand Response and Energy Consumption. *Appl. Energy* **2024**, *356*, 122359. [CrossRef]
4. Miao, Y.; Ye, T.; Xiao, J.; Lau, S.S.Y.; Zhou, Z. Investigation on Alkali-Activated Insulation Mortar Containing High-Volume Recycled Concrete Powder for Energy-Efficient Buildings. *Energy Build.* **2024**, *303*, 113825. [CrossRef]
5. O'Hegarty, R.; Amedeo, G.; Kinnane, O. The Impact of Compromised Insulation on Building Energy Performance. *Energy Build.* **2024**, *316*, 114337. [CrossRef]
6. Mirnezami, S.; Hassani, A.; Baya, A. Evaluation of the Effect of Metallurgical Aggregates (Steel and Copper Slag) on the Thermal Conductivity and Mechanical Properties of Concrete in Jointed Plain Concrete Pavements (JPCP). *Constr. Build. Mater.* **2023**, *367*, 129532. [CrossRef]
7. López-Rebollo, J.; Del Pozo, S.; Nieto, I.M.; Blázquez, C.S.; González-Aguilera, D. Experimental Study on the Thermal Properties of Pigmented Mortars for Use in Energy Efficiency Applications. *J. Clean. Prod.* **2023**, *382*, 135280. [CrossRef]
8. Rashid, F.L.; Al-Obaidi, M.A.; Dulaimi, A.; Bernardo, L.F.A.; Eleiwi, M.A.; Mahood, H.B.; Hashim, A. A Review of Recent Improvements, Developments, Effects, and Challenges on Using Phase-Change Materials in Concrete for Thermal Energy Storage and Release. *J. Compos. Sci.* **2023**, *7*, 352. [CrossRef]
9. Yan, L.; Yaghmour, E.; Scott, D.; Abu Qamar, M.I.; Fox, J.; Naito, C.; Neti, S.; Romero, C.E.; Sarunac, N.; Suleiman, M. Experimental Investigation of the Thermal Performance of Pervious Concrete Integrated with Phase Change Material for Dry Cooling Applications. *Appl. Therm. Eng.* **2024**, *23*, 121749. [CrossRef]
10. Li, L.; Joseph, P.; Zhang, X.; Zhang, L. A Study of Some Relevant Properties of Concrete Incorporating Waste Ceramic Powder as a Cement Replacement Agent. *J. Build. Eng.* **2024**, *87*, 109106. [CrossRef]
11. Haigh, R.; Sandanayake, M.; Sasi, S.; Yaghoubi, E.; Joseph, P.; Vrcelj, Z. Microstructural Attributes and Physiochemical Behaviours of Concrete Incorporating Various Synthetic Textile and Cardboard Fibres: A Comparative Review. *J. Build. Eng.* **2024**, *86*, 108690. [CrossRef]
12. Chen, C.; Liu, X.; Liu, Z.; Shao, L.; Chang, H.; Liu, Q.; Miao, C.; Feng, P. Developing Heat-Conductive Concrete with Graphite-Modified Recycled Aggregates. *Compos. Part B Eng.* **2024**, *284*, 111721. [CrossRef]
13. Gautam, A.; Tung, S. Advancing Sustainability in Concrete Construction: Enhancing Thermal Resilience and Structural Strength with Ground Granulated Blast Furnace Slag. *Asian J. Civ. Eng.* **2024**, *25*, 6119–6129. [CrossRef]
14. Bai, Y.H.; Xie, Y.L.; Chen, Y. Innovative Multi-Functional Foamed Concrete Made from Rice Husk Ash: Thermal Insulation and Electromagnetic Wave Absorption. *J. Mater. Sci.* **2024**, *59*, 16112–16128. [CrossRef]
15. Gedik, E.; Atmaca, A. An Experimental Study Investigating the Effects of Bentonite Clay on Mechanical and Thermal Properties of Concrete. *Constr. Build. Mater.* **2023**, *383*, 131279. [CrossRef]
16. Lan, X.L.; Zhu, H.S.; Zeng, X.H.; Long, G.C.; Xie, Y.J. How Nano-Bubble Water and Nano-Silica Affect the Air-Voids Characteristics and Freeze-Thaw Resistance of Air-Entrained Cementitious Materials at Low Atmospheric Pressure? *J. Build. Eng.* **2023**, *69*, 106179. [CrossRef]
17. Priyatham, B.; Lakshmayya, M.T.S.; Chaitanya, D. Review on Performance and Sustainability of Foam Concrete. *Mater. Today Proc.* **2023**, *in press*. [CrossRef]
18. Xu, T.; Garrecht, H. Effects of Mixing Techniques and Material Compositions on the Compressive Strength and Thermal Conductivity of Ultra-Lightweight Foam Concrete. *Materials* **2024**, *17*, 2640. [CrossRef]
19. Abdellatief, M.; Ahmed, Y.M.; Taman, M.; Elfadaly, E.; Tang, Y.; Abadel, A.A. Physico-Mechanical, Thermal Insulation Properties, and Microstructure of Geopolymer Foam Concrete Containing Sawdust Ash and Egg Shell. *J. Build. Eng.* **2024**, *90*, 109374. [CrossRef]
20. Bong, S.H.; Du, H. Sustainable Additive Manufacturing of Concrete with Low-Carbon Materials. In *Sustainable Concrete Materials and Structures*; Woodhead Publishing: Sawston, UK, 2024; pp. 317–341. [CrossRef]
21. Beytekin, H.E.; Kaya, Y.; Mardani, A.; Sezer, F.Ş. Effect of Fiber Type, Size, and Utilization Rate on Mechanical and Thermal Properties of Lightweight Concrete Facade Panels. *Struct. Concr.* **2024**, *25*, 3824–3840. [CrossRef]
22. Nguyen-Van, V.; Tran, P.; San Ha, N.; Xie, Y.M.; Aslani, F. Blast Resistance of 3D-Printed Bouligand Concrete Panels Reinforced with Steel Fibers: Numerical Investigations. *Compos. Struct.* **2024**, *348*, 118481. [CrossRef]
23. Ma, W.; Kolb, T.; Rüther, N.; Meinlschmidt, P.; Chen, H.; Yan, L. Physical, Mechanical, Thermal and Fire Behaviour of Recycled Aggregate Concrete Block Wall System with Rice Husk Insulation. *Energy Build.* **2024**, *320*, 114560. [CrossRef]
24. Mohamed, A.M.; Tayeh, B.A.; Majeed, S.S.; Aisheh, Y.I.A.; Salih, M.N.A. Ultra-Light Foamed Concrete Mechanical Properties and Thermal Insulation Perspective: A Comprehensive Review. *J. CO2 Util.* **2024**, *83*, 102827. [CrossRef]
25. Salehpour, B.; Ghobadi, M.; Ge, H.; Moore, T. Effects of Thermal Mass on Transient Thermal Performance of Concrete-Based Walls and Energy Consumption of an Office Building. *J. Build. Phys.* **2023**, *47*, 92–120. [CrossRef]
26. Gbekou, F.K.; Belloum, R.; Chennouf, N.; Agoudjil, B.; Boudenne, A.; Benzarti, K. Thermal Performance of a Building Envelope Including Microencapsulated Phase Change Materials (PCMs): A Multiscale Experimental and Numerical Investigation. *Build. Environ.* **2024**, *253*, 111294. [CrossRef]
27. Mendes, V.F.; Cruz, A.S.; Gomes, A.P.; Mendes, J.C. A Systematic Review of Methods for Evaluating the Thermal Performance of Buildings through Energy Simulations. *Renew. Sustain. Energy Rev.* **2024**, *189*, 113875. [CrossRef]
28. Uribe, D.; Vera, S.; Perino, M. Development and Validation of a Numerical Heat Transfer Model for PCM Glazing: Integration to EnergyPlus for Office Building Energy Performance Applications. *J. Energy Storage* **2024**, *91*, 112121. [CrossRef]

29. Ding, X.; Yu, J.; Lin, J.; Chen, Z.; Li, J. Experimental Investigations of Prefabricated Lightweight Self-Insulating Foamed Concrete Wall Panels. *Structures* **2024**, *61*, 106001. [CrossRef]
30. Shi, J.; Zhang, M.; Zhu, X.; Yalçınkaya, Ç.; Çopuroğlu, O.; Liu, Y. Evaluation of Thermal Insulation Capacity and Mechanical Performance of a Novel Low-Carbon Thermal Insulating Foam Concrete. *Energy Build.* **2024**, *323*, 114744. [CrossRef]
31. Nilimaa, J. Smart materials and technologies for sustainable concrete construction. *Dev. Built Environ.* **2023**, *15*, 100177. [CrossRef]
32. Patel, B.; Rathore, P.K.S.; Gupta, N.K.; Sikarwar, B.S.; Sharma, R.; Kumar, R.; Pandey, A. Location optimization of phase change material for thermal energy storage in concrete block for development of energy efficient buildings. *Renew. Energy* **2023**, *218*, 119306. [CrossRef]
33. Acar, M.C.; Çelik, A.I.; Kayabaşı, R.; Şener, A.; Özdöner, N.; Özkılıç, Y.O. Production of perlite-based-aerated geopolymer using hydrogen peroxide as eco-friendly material for energy-efficient buildings. *J. Mater. Res. Technol.* **2023**, *24*, 81–99. [CrossRef]
34. Raja, P.; Murugan, V.; Ravichandran, S.; Behera, L.; Mensah, R.A.; Mani, S.; Kasi, A.; Balasubramanian, K.B.N.; Sas, G.; Vahabi, H.; et al. A Review of Sustainable Bio-Based Insulation Materials for Energy-Efficient Buildings. *Macromol. Mater. Eng.* **2023**, *308*, 2300086. [CrossRef]
35. Cuce, E.; Cuce, P.M.; Alvur, E.; Yilmaz, Y.N.; Saboor, S.; Ustabas, I.; Linul, E.; Asif, M. Experimental performance assessment of a novel insulation plaster as an energy-efficient retrofit solution for external walls: A key building material towards low/zero carbon buildings. *Case Stud. Therm. Eng.* **2023**, *49*, 103350. [CrossRef]
36. Nwokediegwu, Z.Q.S.; Ilojianya, V.I.; Ibekwe, K.I.; Adefemi, A.; Etukudoh, E.A.; Umoh, A.A. Advanced materials for sustainable construction: A review of innovations and environmental benefits. *Eng. Sci. Technol. J.* **2024**, *5*, 201–218. [CrossRef]
37. Yu, K.; Jia, M.; Tian, W.; Yang, Y.; Liu, Y. Enhanced thermo-mechanical properties of cementitious composites via red mud-based microencapsulated phase change material: Towards energy conservation in building. *Energy* **2024**, *290*, 130301. [CrossRef]
38. Abdellatief, M.; Elrahman, M.A.; Alanazi, H.; Abadel, A.A.; Tahwia, A. A state-of-the-art review on geopolymer foam concrete with solid waste materials: Components, characteristics, and microstructure. *Innov. Infrastruct. Solut.* **2023**, *8*, 230. [CrossRef]
39. *ASTM C260-86*; Standard Specification for Air-Entraining Admixtures for Concrete. ASTM: West Conshohocken, PA, USA, 1995.
40. *BS EN 12390-3:2019*; Testing Hardened Concrete. Compressive Strength of Test Specimens. BSI: London, UK, 2019.
41. *ISO 8301*; Thermal Insulation–Determination of Steady-State Thermal Resistance and Related Properties–Heat Flow Meter Apparatus. ISO: Genève, Switzerland, 1991.